Title
Understanding the Effect of Cation Disorder on the Voltage Profile of Lithium Transition-Metal Oxides

Journal
Chemistry of Materials, 28(15)

ISSN
0897-4756

Authors
Abdellahi, Aziz
Urban, Alexander
Dacek, Stephen
et al.

Publication Date
2016-08-09

DOI
10.1021/acs.chemmater.6b01438

Peer reviewed

CHEMISTRY OF MATERIALS

Article

pubs.acs.org/cm

Understanding the Effect of Cation Disorder on the Voltage Profile of Lithium Transition-Metal Oxides

Aziz Abdellahi,[†] Alexander Urban,[‡,§] Stephen Dacek,[†] and Gerbrand Ceder*[,‡,§]

[†]Department of Materials Science and Engineering, Massachusetts Institute of Technology, Cambridge, Massachusetts 02141, United States

[‡]Department of Materials Science and Engineering, UC Berkeley, Berkeley, California 94720, United States

[§]Materials Science Division, Lawrence Berkeley National Laboratory, Berkeley, California 94720, United States

Supporting Information

ABSTRACT: Cation disorder is a phenomenon that is becoming increasingly important for the design of high-energy lithium transition metal oxide cathodes ($LiMO_2$) for Li-ion batteries. Disordered Li-excess rocksalts have recently been shown to achieve high reversible capacity, while *in operando* cation disorder has been observed in a large class of ordered compounds. The voltage slope $\left(\frac{dV}{dx_{Li}}\right)$ is a critical quantity for the design of cation-disordered rocksalts, as it controls the Li capacity accessible at voltages below the stability limit of the electrolyte (~4.5−4.7 V). In this study, we develop a lattice model based on first principles to understand and quantify the voltage slope of cation-disordered $LiMO_2$. We show that cation disorder increases the voltage slope of Li transition metal oxides by creating a statistical distribution of transition metal environments around Li sites, as well as by allowing Li occupation of high-voltage tetrahedral sites. We further demonstrate that the voltage slope increase upon disorder is generally smaller for high-voltage transition metals than for low-voltage transition metals due to a more effective screening of Li−M interactions by oxygen electrons. Short-range order in practical disordered compounds is found to further mitigate the voltage slope increase upon disorder. Finally, our analysis shows that the additional high-voltage tetrahedral capacity induced by disorder is smaller in Li-excess compounds than in stoichiometric $LiMO_2$ compounds.

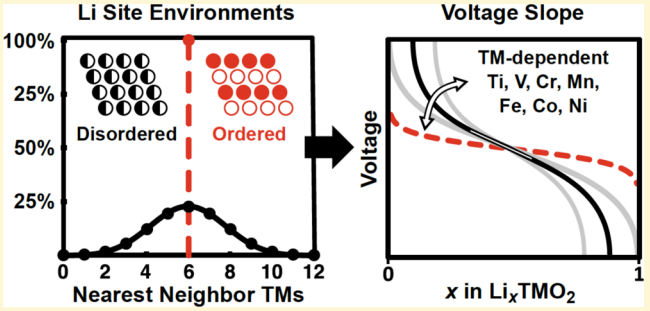

1. INTRODUCTION

Cation disorder is a phenomenon that is becoming increasingly important in the field of Li-ion batteries. As-synthesized disordered Li-excess rocksalts ($Li_{1+x}Nb_yM_zO_2$ [M = Mn, Fe, Co, Ni],[1,2] $Li_{1.2}Ni_{0.33}Ti_{0.33}Mo_{0.14}O_2$,[3] $Li_{1+x}Ti_{2x}Fe_{1-3x}O_2$[4]) were recently shown to achieve high reversible capacity, paving the way toward a new design space of high-capacity Li-ion battery cathodes. These high capacities are enabled by macroscopic Li transport through percolating zero-transition-metal pathways, which remain active upon disorder.[5,6] In operando cation disorder also occurs in a large class of ordered materials, resulting in the formation of disordered bulk phases ($Li_{1.211}Mo_{0.467}Cr_{0.3}O_2$,[5] Li_2VO_3,[7] $LiCrO_2$,[8,9] $Li_{0.96}VO_2$,[10] rutile TiO_2[11,12]) upon electrochemical cycling. Furthermore, in operando cation disorder can also occur at the surface of ordered compounds as a result of oxygen loss and transition metal migration, such as is the case for the NCA ($LiNi_{0.8}Co_{0.15}Al_{0.05}O_2$)[13,14] and Li-excess NMC ($Li_{1+y}Ni_wCo_zMn_{2-y-w-z}O_2$) compounds.[15−19]

Understanding the effect of cation disorder on the voltage profile of transition metal oxides is therefore critical, both to rationally design high-capacity disordered Li-excess rocksalts as well as to predict the voltage evolution of ordered materials subject to in operando bulk or surface cation disorder.

Cation disorder is expected to increase the voltage slope of lithium transition metal oxides, as Li sees a variety of local transition metal environments in a disordered structure and, hence, a large variety of local Li chemical potentials. The (average) voltage slope, $\frac{dV}{dx_{Li}}$, is a critical quantity for the design of cation-disordered rocksalts, as it controls the capacity accessible at voltages below the stability limit of the electrolyte (nominally 4.5 V to 4.7 V for standard organic electrolytes[20]).

In this study, we develop first principles models to understand the magnitude and the factors that control the voltage slope of cation-disordered rocksalts. The effect of cation disorder on transition metals undergoing a $3^+/4^+$ redox reaction is investigated through a systematic study of first-row $LiMO_2$ compounds (M = Ti, V, Cr, Mn, Fe, Co, Ni). Among these compounds, $LiTiO_2$ and $LiFeO_2$ are known to disorder at solid-state synthesis temperature[21] while $LiVO_2$[10] and $LiCrO_2$[8,9] can

Received: April 11, 2016
Revised: July 7, 2016
Published: July 13, 2016

DOI: 10.1021/acs.chemmater.6b01438
Chem. Mater. 2016, 28, 5373−5383

disorder upon cycling at room temperature. Co and Ni, although not found to disorder in the stoichiometric $LiMO_2$ form, disorder as part of the mixed transition metal systems ($LiM_{0.5}Ti_{0.5}O_2$ compounds, where M = Mn, Fe, Co, Ni).[22−25]

Our work demonstrates that the increase in voltage slope upon cation disorder is induced by a statistical distribution of Li site energies and by the occupancy of tetrahedral sites by Li. We further show that practical cation-disordered materials are still short-range ordered and thus exhibit a lower voltage slope than idealized fully disordered compounds with a random cation arrangement. Finally, we demonstrate that the voltage slope increase upon disorder is generally smaller for high-voltage transition metals than for low-voltage transition metals and that the additional tetrahedral capacity resulting from disorder is smaller in Li-excess compounds than in stoichiometric compounds. This study therefore provides critical insights for the design of high-capacity Li-excess cation-disordered rocksalts.

2. MODEL

Cation disorder is defined as cation mixing between the transition metal sublattice and the Li sublattice of an initially ordered structure (e.g., the layered structure of Figure 1a(i)). In the limit of ideally (i.e., fully) disordered $LiMO_2$ rocksalts, Li and M randomly occupy cation sites in the rocksalt lattice (Figure 1a(iii)). In structures with short-range order (Figure 1a(ii)), cation mixing between the Li and M sublattices results in loss of the long-range order, but a short-ranged statistical correlation between the occupancy of nearby sites remains, making the structure different from one with fully randomly occupied sites.[26] In the following, we will therefore distinguish between short-range ordered and fully disordered (i.e., random) structures.

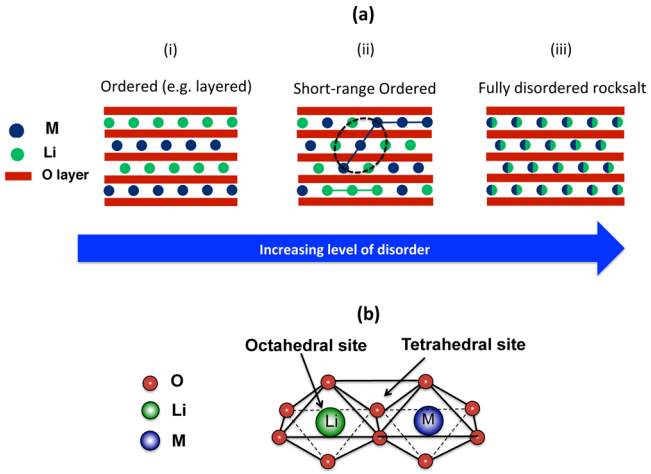

Figure 1. (a) Different levels of cation disorder in $LiMO_2$ compounds. (i) Fully ordered (e.g., layered) $LiMO_2$ compound (the layers being the (111) planes of the FCC cation sublattice). (ii) Short-range ordered and (iii) fully disordered rocksalt (random cation arrangement). (b) Cation coordination in the rocksalt structure.

Figure 1b illustrates the cation coordination in the rocksalt structure. In fully lithiated $LiMO_2$, all cations (Li and M) are octahedrally coordinated by oxygen, regardless of whether the structure is ordered or disordered. In disordered structures, Li may further occupy tetrahedral sites upon delithiation, under conditions that will be detailed below. Note that each tetrahedral site shares faces with four adjacent octahedral cation sites (for clarity, Figure 1b only illustrates two of these face-sharing octahedra) and that there are two tetrahedral sites per octahedral site.

In the following section, we outline the factors that contribute to the voltage slope of cation-disordered rocksalts. We define the voltage slope as the change of the voltage V with Li concentration x_{Li} which can equivalently be expressed in terms of the curvature of the formation free energy (per formula unit of Li) G_f:

$$\frac{dV}{dx_{Li}} = -\frac{d^2G_f}{(dx_{Li})^2} \tag{1}$$

We further define the average voltage slope in a concentration range $[x_{Li}^1, x_{Li}^2]$ as

$$\left\langle \frac{dV}{dx_{Li}} \right\rangle_{[x_{Li}^1, x_{Li}^2]} = \frac{V(x_{Li}^1) - V(x_{Li}^2)}{(x_{Li}^2 - x_{Li}^1)} \tag{2}$$

We begin this discussion by considering the factors that control the voltage slope in ordered (e.g., layered) $LiMO_2$ compounds. We define the site energy, ΔE_{site}, as the change of energy solely due to Li−M interactions when Li is extracted from (or inserted to) a particular Li site in the structure. Using this definition, the site energy does not depend on the interaction between adjacent Li sites. In the layered structure, each Li site sees the same local transition metal environment (6 out of the 12 nearest neighbor cation sites are occupied by M). As a result, the site energy is uniform across all Li sites in the structure. In the absence of interactions between adjacent Li sites, the Li−vacancy (Li−Va) binary system would be an ideal solution, controlled solely by entropic effects. The formation free energy of an ideal solution, $G_f(x_{Li})$, is small at room temperature ($|G_f(x_{Li})| = -kT(x_{Li}\ln(x_{Li}) + (1 - x_{Li})\ln(1 - x_{Li})) < 25$ meV/f.u.). The corresponding voltage slope is also small: $\left.\frac{dV}{dx_{Li}}\right|_{x_{Li}=0.5} = -\left.\frac{d^2G_f}{(dx_{Li})^2}\right|_{x_{Li}=0.5} = -4$ kT ≈ 0.1 V. In practice, the voltage slope of the layered structure is therefore controlled by the interaction between adjacent Li sites, or more rigorously by the *effective Li−Va interaction* (J^{Li-Va}). This quantity describes the energy of adjacent Li−Va pairs compared to phase-separated Li−Li and Va−Va pairs ($-2J^{Li-Va} = [E^{Li-Va} - 0.5(E^{Li-Li} + E^{Va-Va})] < 0$). The effective Li−Va interaction, when positive, makes states of intermediate Li concentration thermodynamically favorable over a linear combination of the $LiMO_2$ and MO_2 end members (Figure 2a(i)), which in turn increases the voltage slope. Thus, the stronger the interaction between Li sites, the larger the voltage slope becomes (Figure 2a(ii)).

We now consider the additional factors that contribute to the voltage slope in disordered structures. Cation disorder creates a statistical distribution of local transition metal environments around Li sites. Figure 2b(i) (black curve) shows for the random structure the probability that, out of the 12 nearest neighbors of a given Li atom, Z^M are transition metals. This variety of local environments results in a distribution of Li site energies controlled by the effective Li−M interaction and characterized by a standard deviation $\sigma_{\Delta E_{site}}$. This is in contrast to the layered structure, where each Li site sees the same transition metal coordination (6 out of the 12 nearest neighbor cation sites are occupied by M, as indicated by the red circle in

DOI: 10.1021/acs.chemmater.6b01438
Chem. Mater. 2016, 28, 5373−5383

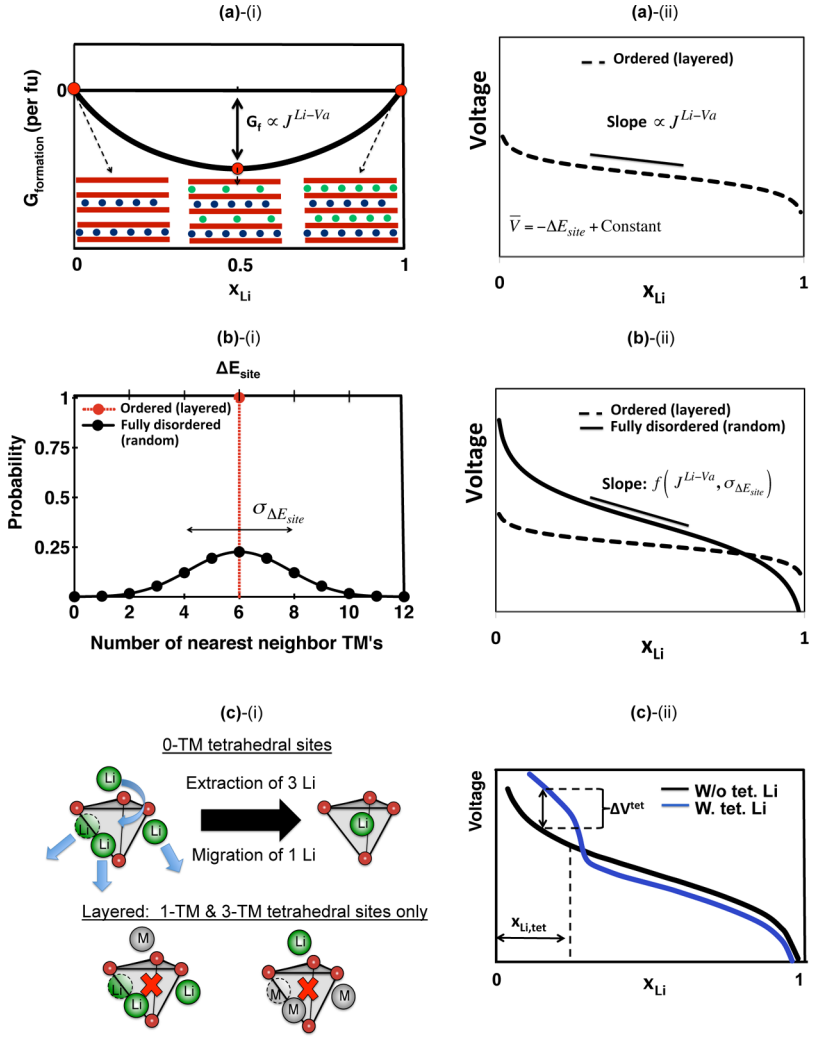

Figure 2. Factors that contribute to the increase of the voltage slope upon cation disorder in lithium transition metal oxides. (a) In ordered (e.g., layered) compounds, the effective Li–Va interaction ($J^{\mathrm{Li-Va}}$) controls the change of energy with concentration (i), which in turn controls the voltage slope (ii). (b) In disordered compounds, (i) the statistical distribution of local environments around Li sites results in a statistical distribution of ΔE_{site}, and (ii) both $J^{\mathrm{Li-Va}}$ and $\sigma_{\Delta E_{\mathrm{site}}}$ (the standard deviation of ΔE_{site}) contribute to the voltage slope. (c) High-voltage tetrahedral sites can be occupied by Li when all face-sharing octahedral sites are vacant. (i) This can occur in disordered $LiMO_2$ compounds via delithiation of "0-TM" tetrahedral sites, but not in the (stoichiometric) layered structure, as each tetrahedral site has at least one transition metal neighbor. (ii) Tetrahedral Li occupancy leads to a voltage increase at the end of charge and a corresponding lowering of the voltage everywhere else to conserve the average voltage.

Figure 2b(i)). In disordered structures, the net voltage slope is therefore a combination of both the site energy distribution and the effective Li–Va interaction, as illustrated in Figure 2b(ii), and as a result, disordering a layered compound is expected to lead to a voltage slope increase.

Cation disorder also leads to occupancy of high-voltage tetrahedral sites by Li at high states of charge (Figure 2c). Tetrahedral sites are energetically favorable over octahedral sites if all face-sharing octahedral sites are vacant (referred to as the "0-TM" condition).[5,6] Occupancy of tetrahedral sites by Li creates a high-voltage region in the voltage profile, as has been observed in cation-mixed $LiNi_{0.5}Mn_{0.5}O_2$[27] and spinel Li_xMnO_2 (in the x = [0, 0.5] range[28]). After extraction of three out of four face-sharing Li around such 0-TM tetrahedral sites (Figure 2c(i)), the remaining Li migrates into the tetrahedral site, from where it requires a higher voltage to be extracted. The 0-TM condition is never met in the (stoichiometric) layered structure, as each tetrahedral site has at least one transition metal neighbor (Figure 2c(i)). Cation disorder, however, creates a statistical distribution of metal environments around tetrahedral sites, such that the 0-TM condition is met with a certain probability. The effect of tetrahedral occupancy on the voltage profile of cation-disordered rocksalts is schematically illustrated in Figure 2c(ii). Note that the presence of a high-voltage region at the end of charge is accompanied by a lowering of the voltage everywhere else, to conserve the average voltage (which only depends on the free energy of the $LiMO_2$ and MO_2 end members).

In order to quantitatively evaluate the voltage slope of cation-disordered rocksalts, the standard deviation of the site energy distribution, the effective Li–Va interaction, and the high-voltage capacity resulting from tetrahedral Li occupancy are evaluated from first principles. Cluster expansions based on pair interactions are developed to evaluate the voltage slope arising from Li insertion in octahedral sites (capturing the combined effect of the site energy distribution and the effective Li–Va

DOI: 10.1021/acs.chemmater.6b01438
Chem. Mater. 2016, 28, 5373–5383

interaction), while the additional effect of tetrahedral Li occupancy on the voltage profile ($x_{\mathrm{Li,tet}}$ and ΔV^{tet} in Figure 2c) is estimated from probability theory and from first principles energy evaluations. These methods are detailed in the following paragraphs.

Cluster expansions[29−33] provide a mathematical framework to map the energy of any Li−M−Va configuration in disordered Li_xMO_2 onto a finite set of Effective Cluster Interactions (ECIs). As such, they have been used to calculate the phase diagram and voltage profiles of Li_xMO_2[34,35] or the dependence of the average voltage on Li−M configurations.[36] In this work, pairwise cluster expansions are used to evaluate the voltage slope associated with Li insertion into octahedral sites. In order to take advantage of the cluster expansion framework, the site energy $\Delta E^i_{\mathrm{site}}$ and the interaction between adjacent Li sites are expressed in terms of Effective Cluster Interactions, which are then fitted to a set of energies obtained from first principles.

Under a pair term approximation, the energy landscape in a Li−M−Va system is entirely described by three effective cluster interactions: the effective Li−M interaction ($J^{\mathrm{Li-M}}$), the effective Va−M interaction ($J^{\mathrm{Va-M}}$), and the effective Li−Va interaction ($J^{\mathrm{Li-Va}}$), which we described above. These effective interactions can be expressed as combinations of all possible pair energies on the lattice ($E^{\mathrm{Li-M}}$, $E^{\mathrm{Va-M}}$, $E^{\mathrm{Li-Va}}$, $E^{\mathrm{Li-Li}}$, $E^{\mathrm{Va-Va}}$, $E^{\mathrm{M-M}}$ [37]).

$$-2J^{\mathrm{A-B}} = \left[E^{\mathrm{A-B}} - \frac{(E^{\mathrm{A-A}} + E^{\mathrm{B-B}})}{2}\right] \tag{3}$$

where A and B can be either Li, M, or Va. Now consider a disordered rocksalt in which the distribution of transition metals over octahedral sites is random and does not change upon cycling. Limiting the interaction between Li sites to the nearest neighbor shell, the energy of a given Li distribution (σ) can be written as

$$E(\sigma) = \sum_i \frac{\Delta E^i_{\mathrm{site}}}{2}\sigma_i + \sum_{i,j\in nn\,\mathrm{pairs}} J^{\mathrm{Li-Va}}_{nn}\sigma_i\sigma_j \tag{4}$$

where σ_i is the occupation of site i on the Li/Va sublattice (σ_i = {1, −1} for {Li, Va}), $\Delta E^i_{\mathrm{site}}$ is the site energy of site i, and $J^{\mathrm{Li-Va}}_{nn}$ is the interaction term between adjacent Li sites, which captures the preference for Li−Va pairs over phase-separated Li−Li and Va−Va pairs as described above. Note that the factor of 1/2 in the first term of eq 4 is simply a consequence of the σ_i = {1, −1} convention for {Li, Va} occupancy.

The site energy $\Delta E^i_{\mathrm{site}}$ is defined as the Li insertion energy when adjacent Li sites do not interact with each other ($J^{\mathrm{Li-Va}}_{nn}$ = 0) and depends on the relative strength of the effective Li−M and Va−M interactions via the following relation (see Supporting Information for a detailed derivation):

$$\Delta E^i_{\mathrm{site}} = \sum_{\mathrm{Neighbor\,shell}\,k} [-2Z^{\mathrm{M},(i)}_k(J^{\mathrm{Li-M}}_k - J^{\mathrm{Va-M}}_k)] + C \tag{5}$$

where the subscript k denotes the kth neighbor shell, Z_k is the total coordination number of the kth neighbor shell, $Z^{\mathrm{M},(i)}_k$ is the number of transition metals around site i in the kth neighbor shell, and C is a constant chemical potential shift that defines the chemical potential reference. The site energy therefore emerges as the difference between the effective Li−M interaction and the effective Va−M interaction over several neighbor shells, which we will simply refer to as the "effective Li−M interaction" from now on. After obtaining suitable values for $J^{\mathrm{Li-Va}}$, $J^{\mathrm{Li-M}}_k$, and $J^{\mathrm{Va-M}}_k$, the lattice model can be combined with Monte Carlo simulations to determine the open circuit voltage profile $V(x_{\mathrm{Li}})$ and hence the voltage slope $\frac{\mathrm{d}V}{\mathrm{d}x_{\mathrm{Li}}}$. We define the average octahedral-site voltage slope by performing a linear fit to the voltage curve in the x_{Li} = [0.25, 0.75] capacity range.

$J^{\mathrm{Li-Va}}_{nn}$ is fitted to the average voltage slope of the layered structure over the x_{Li} = [0, 1] concentration (T = 0 limit), as calculated within the Hubbard-U corrected Generalized Gradient Approximation (GGA+U) to Density Functional Theory (DFT), using the PBE exchange-correlation functional.[38−40] The U values are taken from the work of Jain et al.[41] $J^{\mathrm{Li-M}}$ and $J^{\mathrm{Va-M}}$ are obtained by fitting two pair-based cluster expansions: one for Li/M arrangements at the $LiMO_2$ composition and one for Va/M arrangements at the MO_2 composition. The structure set over which the fit is performed is the set of all periodic cation-mixed structures with unit cells containing up to eight cations. The fits are obtained within the compressive sensing paradigm, using the split Bregman algorithm,[32] by considering pair interactions up to the fifth neighbor. More details on the methodology are provided in the Supporting Information.

In this study, we limit the lattice model for Li insertion into octahedral sites to pair interactions. The accuracy of this approximation can be assessed by comparing the predictions of the pair term model with alternate methods using higher order interactions (see Supporting Information). We find that the pair term model correctly predicts the (site-energy induced) voltage slope of fully disordered $LiMO_2$ to within 0.2 V, which leads to an uncertainty of 0.1 V in the high voltage limit and therefore constitutes a good approximation (Figure S1).

We further estimate the additional voltage step induced by tetrahedral Li occupancy (ΔV^{tet} in Figure 2c(ii)) by calculations on the spinel structure. The topology of the spinel structure is such that at x_{Li} = 0.5 in Li_xMO_2, all Li atoms occupy 0-TM tetrahedral sites.[28] Using Density Functional Theory, we can compare the voltage profile arising from tetrahedral occupancy with the voltage profile arising from octahedral Li occupancy in the same concentration range. The difference between the two high-voltage plateaus can be used to estimate the voltage slope increase in disordered rocksalts resulting from tetrahedral Li occupancy (ΔV^{tet} in Figure 2c(ii); more details are given in Figure S2 of the Supporting Information). The capacity resulting from tetrahedral Li occupancy ($x_{\mathrm{Li,tet}}$) can then be calculated using probability arguments (method detailed in the Results section).

Using the model described above, the voltage slope can be evaluated for both fully disordered (random) $LiMO_2$ (i.e., structures with random cation distribution) as well as for short-range ordered materials. Monte Carlo annealing is used to determine the degree of short-range order in practical compounds. More details are provided in the Results section.

3. RESULTS

3.1. (Average) Voltage Slope Considering Only Octahedral Li Occupancy. In this section, we consider the contribution of octahedral Li insertion to the voltage slope of fully disordered $LiMO_2$ compounds. We consider separately the effect of the distribution of Li-site energies and the Li−Va interaction.

DOI: 10.1021/acs.chemmater.6b01438
Chem. Mater. 2016, 28, 5373−5383

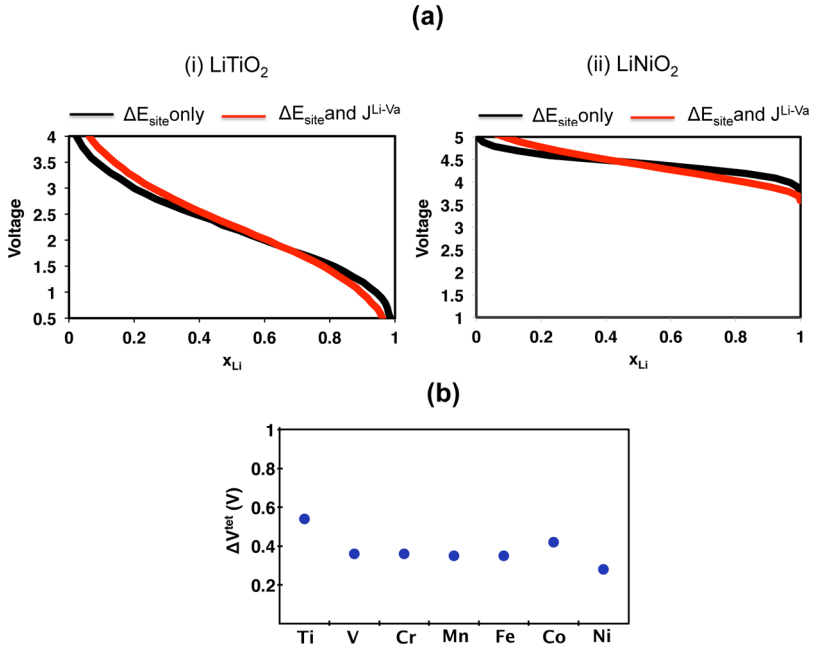

Figure 3. (a) Calculated voltage profile of fully disordered (i) $LiTiO_2$ and (ii) $LiNiO_2$ when Li insertion is restricted to octahedral sites. The black curves show the site energy contribution to the voltage slope, while the red curves show the combined effect of ΔE_{site} and J^{Li-Va}. (b) Estimate of voltage slope increase due to tetrahedral site occupation in disordered $LiMO_2$ (ΔV^{tet} in Figure 2c), as determined from the spinel structure.

Site Energy Distribution. The black curves of Figure 3a illustrate the voltage profiles of $LiTiO_2$ and $LiNiO_2$ when no effective Li−Va interaction is present (note that, as detailed in a previous work,[42] full cation disorder increases the average voltage of $LiTiO_2$ and $LiNiO_2$ compared to their ordered ground-state). The difference in the site energy induced voltage slopes between these compounds is large, suggesting that the site energy contribution to the voltage slope strongly depends on the transition metal. We performed a similar analysis for all transition metals, and the black bars in Figure 4a show the site energy contribution to the voltage slope for the different transition metals. This slope varies between 2.1 V for $LiTiO_2$ and 0.5 V for $LiNiO_2$. The black squares of Figure 4b show the relationship between the site-energy induced voltage slope and the average voltage of disordered $LiMO_2$ compounds. This plot shows that high-voltage transition metals generally have a lower site-energy induced voltage slope than low voltage transition metals. This inverse correlation is favorable for the design of high-voltage cation-disordered rocksalts, as a high average voltage and a low voltage slope are simultaneously desirable to access maximal capacity at high energy. The origin and implication of this inverse correlation are discussed further in the Summary and Discussion section of this paper.

Li−Va Interaction. We now consider the additional effect of the effective Li−Va interaction on the voltage slope of fully disordered $LiMO_2$. We obtain the effective Li−Va interaction from the voltage slope of perfectly layered materials in which no site energy variation is present. The calculated voltage slope of the perfect layered compounds is given in Table 1.

The voltage profile of fully disordered $LiTiO_2$ and $LiNiO_2$, including both the site energy and the effective Li−Va interaction, is shown by the red curves of Figure 3a. The presence of the effective Li−Va interaction increases the voltage slope, while keeping the average voltage constant.

The sum of the black and red bars in Figure 4a shows the voltage slope associated with Li insertion in octahedral sites when both the site energy distribution and the effective Li−Va interaction are taken into account. The effect of the Li−Va interaction on the voltage slope is found to be proportional to the slope of the layered structure reported in Table 1. It is strongest for $LiCrO_2$ (layered slope of 1.05 V) and lowest for $LiMnO_2$ (layered slope of 0.5 V). The strong Li−Va interaction in the Cr system is responsible for the higher octahedral voltage slope of fully disordered $LiCrO_2$ with respect to other high-voltage transition metals (Mn, Fe, Co, Ni) and also accounts for the higher octahedral voltage slope of $LiCrO_2$ with respect to $LiVO_2$, despite $LiVO_2$ having a larger site-energy induced voltage slope due to its lower average voltage.

The red squares of Figure 4b summarize the increase in voltage slope resulting from full disorder of an initially layered $LiMO_2$ compound, illustrated as a function of the average voltage of the fully disordered structure. Much like the site energy contribution to the voltage slope (black squares of Figure 4b), the voltage slope increase upon disorder is found to inversely correlate with the average voltage of the disordered structure. This further indicates that the increase of the octahedral-Li voltage slope is largely attributable to the creation of a site energy distribution resulting from Li−M interactions.

The voltage range over which octahedral Li insertion occurs in fully disordered $LiMO_2$ is illustrated by the red bars of Figure 4c (this voltage range is defined by $\left[\bar{V} - \frac{Slope}{2}, \bar{V} + \frac{Slope}{2}\right]$, where $\bar{V}$ is the average voltage) . As a result of the smaller site energy contribution to the voltage slope, high-voltage transition metal compounds are found to only have a small amount of capacity above the 4.5−4.7 V stability limit of the electrolyte, with the exception of $LiNiO_2$ which has a high average voltage in its fully disordered form.[42] For all transition metals except Ni, cation disorder therefore does not lead to a significant amount of inaccessible octahedral Li capacity. (It is to be noted that, in the case of $LiCrO_2$, disorder also leads to an average voltage decrease of ∼0.3 V with respect to the layered ground

DOI: 10.1021/acs.chemmater.6b01438
Chem. Mater. 2016, 28, 5373−5383

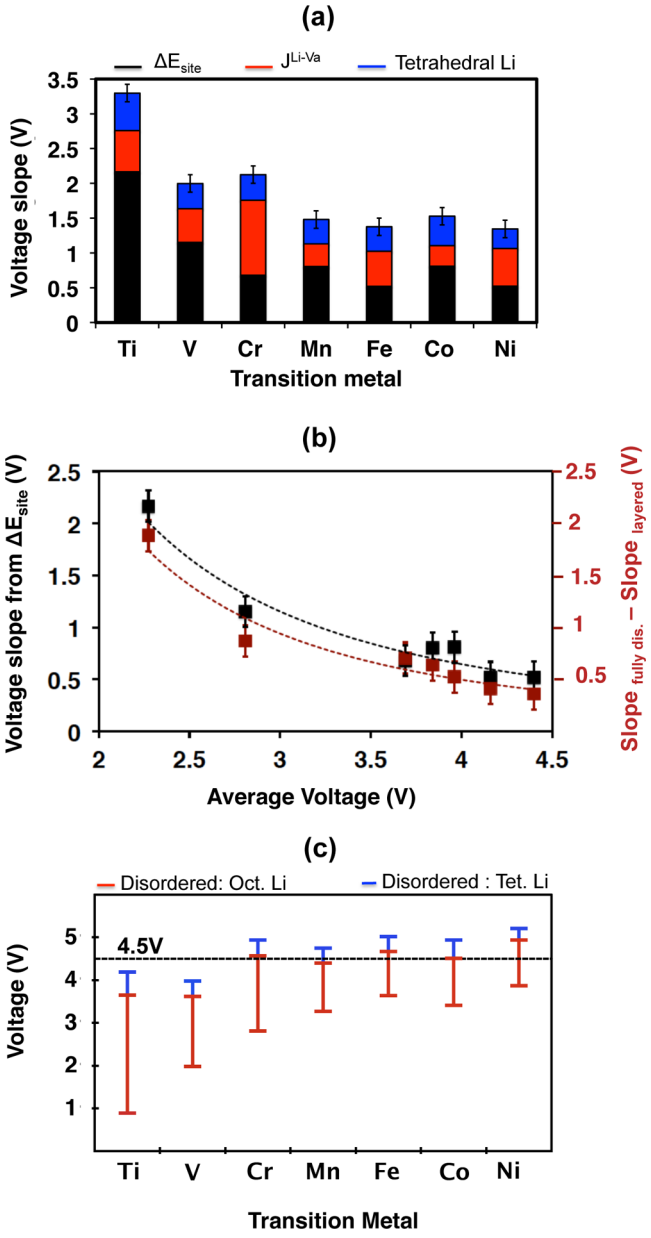

Figure 4. Calculated voltage slope and voltage range of fully disordered $LiMO_2$. (a) Voltage slope contributions from ΔE_{site}, J^{Li-Va}, and tetrahedral Li for each compound (the error bar is evaluated from cluster expansions containing higher order interactions, as described in the Supporting Information). (b) Correlation between the voltage slope increase upon disorder and the average voltage of fully disordered compounds. The black squares denote the site-energy contribution to the voltage slope. High-voltage compounds have a lower (site-energy induced) voltage slope than low-voltage compounds, as evidenced by the black dashed trend line. The red squares illustrate the total voltage slope increase upon full disorder of an initially layered $LiMO_2$ compound when tetrahedral occupancy is excluded. The voltage slope increase inversely correlates with the average voltage, in a manner similar to the site-energy contribution to the voltage slope (red dashed trend line). (c) Voltage range of fully disordered $LiMO_2$. The red bar represents the voltage range associated with octahedral Li insertion $\left(\left[\bar{V} - \frac{Slope}{2}, \bar{V} + \frac{Slope}{2}\right]\right.$, where $\bar{V}$ is the average voltage of the disordered structure), while the blue bar highlights the additional high voltage contribution associated with insertion of Li in tetrahedral sites. The dashed line represents the 4.5 V line, which represents a lower bound for the electrolyte stability limit.

state.[42] This decrease partially accounts for the small capacity observed above 4.5 V in this compound).

3.2. Tetrahedral Li Occupancy. Occupancy of tetrahedral sites by Li is expected to further increase the voltage slope of cation-disordered rocksalts. During delithiation, some Li will migrate from octahedral to tetrahedral sites as its face-sharing Li ions are removed. This lowers the energy increase needed for Li extraction and, hence, decreases the extraction voltage in the initial part of the charge. As the tetrahedral Li sits at lower energy than the octahedral Li, it only becomes extracted at the end of charge at higher voltage. Hence, while occupation of tetrahedral sites by Li in the electrochemical cycle does not change the average voltage, it does increase the slope of the voltage.

Probability arguments can be used to calculate the tetrahedral Li capacity in a fully disordered $LiMO_2$ rocksalt. In a fully lithiated $LiMO_2$ rocksalt, each cation site can be occupied by Li with a probability of 1/2. The probability for a given tetrahedral site to have no face-sharing octahedral M neighbors (the 0-TM condition) is therefore $(1/2)^4$. Furthermore, there are 4 tetrahedral sites per formula unit of $LiMO_2$. The maximal tetrahedral capacity in fully cation-disordered $LiMO_2$ is therefore 0.25 formula units (f.u.) of Li:

$$\text{Tetrahedral Capacity (fully disordered LiMO}_2) = 4\left(\frac{1}{2}\right)^4 = 0.25 \quad (6)$$

Figure 3b shows the voltage difference between Li in the tetrahedral and Li in the octahedral sites as determined from the spinel structure. The resulting voltage increase is found to be on the order of 0.3−0.5 V, depending on the transition metal. For some of the later transition metals where the octahedral voltage is already close to the electrolyte stability limits, this additional voltage increase at the end of charge therefore leads to up to 25% capacity outside the 4.5−4.7 V stability of the electrolyte (blue bars of Figure 4c).

3.3. Short-Range Order. In practice, the cation arrangement in disordered rocksalt is not random but in fact exhibits a certain degree of short-range order.[22] We have investigated short-range order in $LiMO_2$ compounds by studying the Li/M configurations and their energy as a function of temperature. This is made possible by the use of $LiMO_2$ cluster expansions which accurately reproduce the $LiMO_2$ ground-state structure while predicting the energy of any given Li/M ordering to within ~25 meV/cation or less.[42,43]

Using Monte Carlo simulations to thermalize the system, both the energy and the order−disorder transition temperature can be evaluated.[43] For all transition metals, it is found that the energy of thermally equilibrated structure is lower than the energy of the fully random structure, which is shown in the cartoon representation of Figure 5a. These results indicate that a certain amount of short-range order is still present even when the structure is on average disordered into the rocksalt symmetry. In the case of $LiFeO_2$, for example, the energy of the short-range ordered structure (referenced to the ground-state energy) at 300 K above the temperature of the order−disorder transition is only 60% that of the structure with fully random Li/TM occupancies.

Short-range order affects the site energy distribution ($\sigma\Delta_{E_{site}}$ in the random limit) as it removes the extreme environments for Li, corresponding to sites with very low or very high extraction voltage. Short-range order is therefore expected to reduce the voltage slope, with the stronger effect expected in

DOI: 10.1021/acs.chemmater.6b01438
Chem. Mater. 2016, 28, 5373−5383

Table 1. Calculated Voltage Slope (dV/dx_{Li}) of Perfect Layered $LiMO_2$ Compounds Using Density Functional Theory[a]

	$LiTiO_2$	$LiVO_2$	$LiCrO_2$	$LiMnO_2$	$LiFeO_2$	$LiCoO_2$	$LiNiO_2$
slope (V)	0.85 V	0.75 V	1.05 V	0.50 V	0.60 V	0.60 V	0.70 V

[a]The voltage slope is taken to be the average change in voltage over the x_{Li} = [0,1] concentration range, in the $T = 0$ limit.

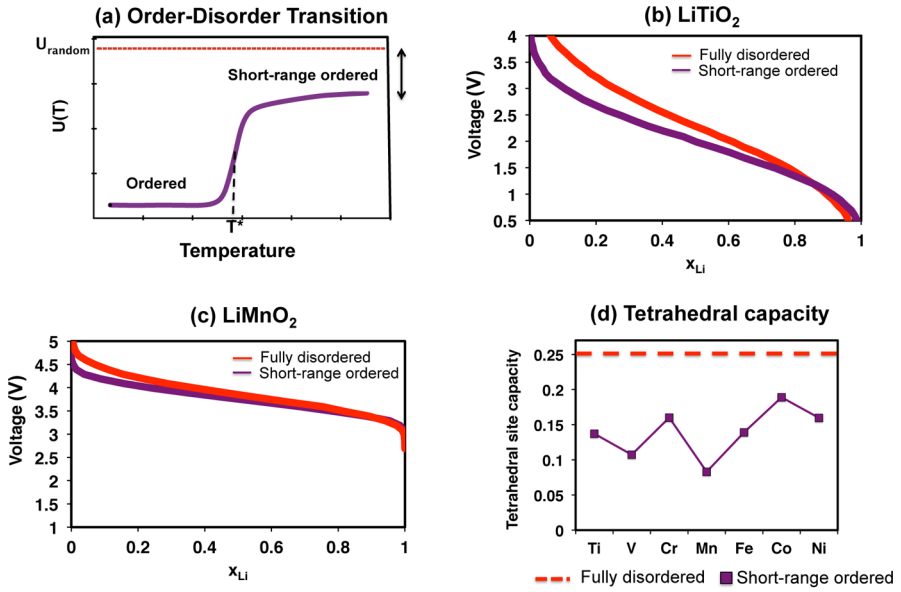

Figure 5. Effect of short-range order on the voltage profile of disordered $LiMO_2$. (a) Schematic indicating that above the order−disorder transition the structure is short-range ordered. (b, c) Voltage profiles of $LiTiO_2$ and $LiMnO_2$ for a cation distribution equilibrated at temperatures above the order−disorder transition temperature. (d) Comparison of tetrahedral Li capacity in fully random and short-range ordered $LiMO_2$ compounds.

compounds that have a large site energy distribution (i.e., low-voltage compounds). To illustrate this, Figure 5b,c shows the voltage profiles of $LiTiO_2$ and $LiMnO_2$ in the random and short-range ordered cases, as obtained from Monte Carlo annealing (octahedral Li insertion only). The short-range ordered configuration was obtained by annealing each system past the order−disorder transition, at a temperature at which the heat capacity dU/dT reaches a value lower than 10^{-5} eV/K per cation (in $LiTiO_2$, for example, this corresponds to $T = T^* + 300$ K). This criterion ensures that the plateau region labeled "disordered" in Figure 5a is accessed. Figure 5b,c demonstrates that the voltage slope decrease resulting from short-range order is much more pronounced for $LiTiO_2$ (slope decrease of 0.8 V) than for $LiMnO_2$ (slope decrease of 0.25 V).

The decrease in voltage slope resulting from short-range order is beneficial for high-voltage transition metals, as it allows for more Li capacity to be accessible below the stability limit of the electrolyte. In fully disordered $LiFeO_2$ and $LiNiO_2$, approximately 0.2 and 0.4 Li per formula unit sit above 4.5 V (considering only octahedral capacity). Short-range order results in an additional ~0.1 Li/f.u. becoming available below 4.5 V in these compounds. For the other high-voltage transition metals (Cr, Mn, Co), minimal octahedral capacity is found above 4.5 V even in the fully random limit (<0.07 Li/f.u.).

Short-range order also decreases the accessible tetrahedral Li capacity with respect to fully disordered compounds for all transition metals. Only those tetrahedral sites that are surrounded by 4 (octahedral) Li sites become stable at low Li content. Hence, the amount of tetrahedral Li at the top of charge, i.e., the tetrahedral capacity, can be estimated by determining the ratio of such 4-Li sites to the total amount of Li in the discharged state. While 25% of the total capacity is accounted for by tetrahedral Li occupancy in $LiMO_2$ with random cation arrangement (Section 3.2), it accounts for only 8−18% in thermally equilibrated disordered compounds (Figure 5d) as determined by Monte Carlo simulations. In general, short-range order therefore leads to more Li capacity accessible below the stability limit of the electrolyte in high-voltage transition metal oxides, via a reduction of the octahedral voltage slope as well as a decrease of available tetrahedral sites.

3.4. Effect of Li Excess on Tetrahedral Capacity. The previous sections have demonstrated that tetrahedral Li capacity can play an important role in determining the high voltage capacity of cation-disordered rocksalts. In practice, cation-disordered rocksalts require Li excess ($y \approx 0.2$ in $Li_{1+y}M_{1-y}O_2$) to sustain macroscopic Li diffusion.[5,6] An important question that needs to be answered is therefore how Li excess affects the relative octahedral and tetrahedral Li capacity in disordered Li-excess rocksalts.

The amount of tetrahedral and octahedral capacity can be obtained as

$$\text{Tetrahedral Capacity (fully disordered } Li_{1+y}M_{1-y}O_2) = 4\left(\frac{1+y}{2}\right)^4 \quad (7)$$

$$\text{Octahedral Capacity (fully disordered } Li_{1+y}M_{1-y}O_2) = (1+y) - 4\left(\frac{1+y}{2}\right)^4 \quad (8)$$

Figure 6b shows the tetrahedral and octahedral capacities as a function of the Li-excess level. Though the potential tetrahedral capacity increases strongly with the amount of Li excess, the concomitant decrease of octahedral Li capacity is small, as the

DOI: 10.1021/acs.chemmater.6b01438
Chem. Mater. 2016, 28, 5373−5383

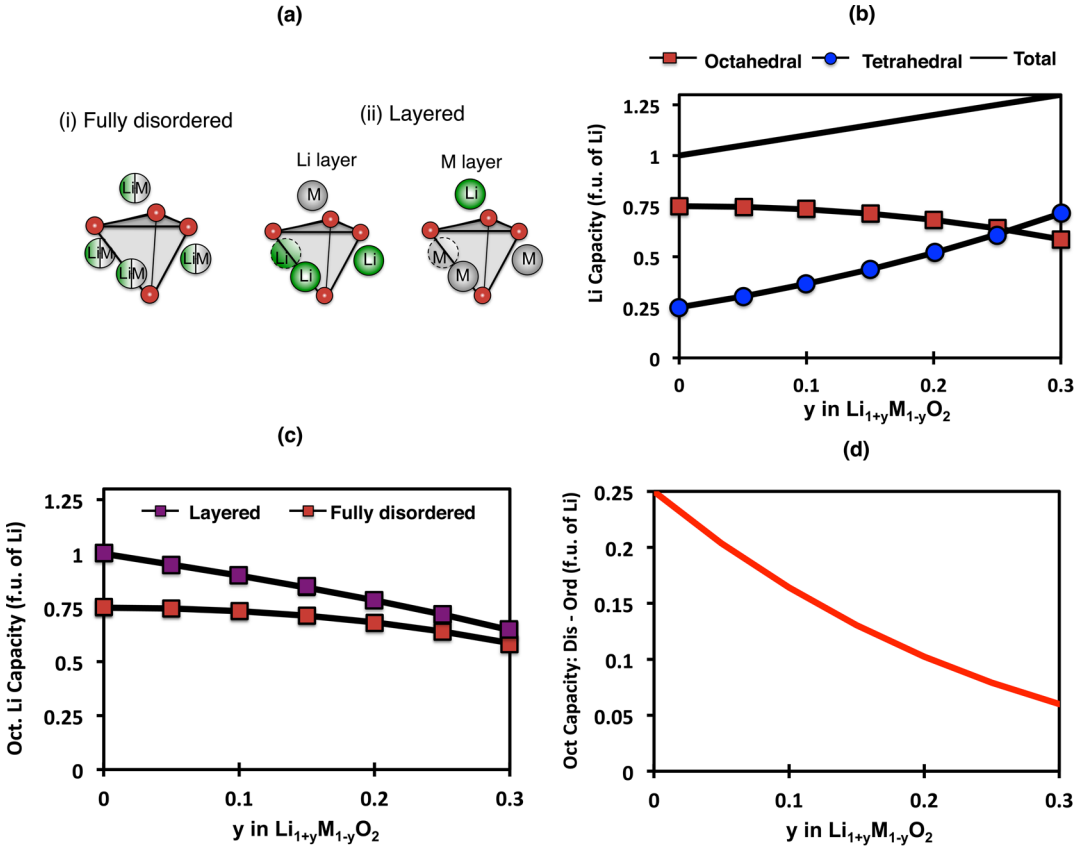

Figure 6. Effect of Li excess on the octahedral and tetrahedral Li capacity in layered and fully disordered $Li_{1+y}M_{1-y}O_2$. (a) Tetrahedral environments in fully disordered and layered $LiMO_2$. (b) Breakdown of the octahedral, tetrahedral, and total Li capacity in fully disordered $Li_{1+y}M_{1-y}O_2$. (c) Octahedral Li capacity as a function Li excess for layered and fully disordered $Li_{1+y}M_{1-y}O_2$. (d) Octahedral capacity lost upon full disorder of initially layered $Li_{1+y}M_{1-y}O_2$ compounds.

total Li content also increases. For example, the octahedral capacity in a fully disordered $Li_{1.2}M_{0.8}O_2$ compound ($y = 0.2$) is smaller than the octahedral capacity in a fully disordered $LiMO_2$ compound by only 0.07 f.u. of Li (Figure 6b). Based on this analysis, to cycle 1 f.u. of Li in a fully disordered $Li_{1.2}M_{0.8}O_2$ compound (~280 mAh/g), about ~90 mAh/g is expected to originate from tetrahedral Li sites.

Furthermore, the amount of octahedral Li capacity lost upon cation disorder decreases as the Li-excess level increases. To show this, we calculate the octahedral capacity in layered $Li_{1+y}M_{1-y}O_2$ and compare it with the octahedral capacity previously obtained for fully disordered $Li_{1+y}M_{1-y}O_2$. In a layered $Li_{1+y}M_{1-y}O_2$ compound, one layer is entirely filled by Li, and the remaining y formula units of Li are distributed in the transition metal layer. In this work, we make the approximation that, in the layered structure, excess Li is randomly distributed in the transition metal layer, such that the probability for a cation site in the M layer to be occupied by Li is simply equal to y. (It is to be noted, however, that the exact structure of layered Li-excess compounds is an object of intense debate in the literature.[17,44] The disappearance of superstructure peaks after the first charge of layered $Li_{1+y}M_{1-y}O_2$,[44] however, suggests that a random distribution of Li site is a reasonable approximation.)

Because of Li excess, some tetrahedral sites will respect the 0-TM condition even in the absence of cation disorder. The total tetrahedral capacity in layered $Li_{1+y}M_{1-y}O_2$ is approximately given by

$$\text{Tetrahedral Capacity (layered } Li_{1+y}M_{1-y}O_2) = 2((1)^3(y) + (1)(y)^3) \quad (9)$$

Note that the factor of 2 accounts for the fact that there are two tetrahedral sites per cation site and that the $(1)^3(y)$ and $(1)(y)^3$ terms quantify the 0-TM probability for tetrahedral sites in the Li and M layers, respectively (cf. Figure 6a(ii)). Finally, the octahedral capacity in layered $Li_{1+y}M_{1-y}O_2$ is

$$\text{Octahedral Capacity (layered } Li_{1+y}M_{1-y}O_2) = (1 + y) - 2[(1)^3(y) + (1)(y)^3] \quad (10)$$

Figure 6c compares the octahedral capacity in layered and fully disordered $Li_{1+y}M_{1-y}O_2$ (via eqs 8 and 10). In both cases, the octahedral capacity decreases with Li excess. But interestingly, the difference in octahedral capacity between the layered and the fully disordered structure also decreases with the amount of Li excess. This is illustrated in Figure 6d, which shows the octahedral capacity lost upon full disorder of an initially layered structure, as a function of Li excess. While 0.25 f.u. of octahedral capacity is lost to tetrahedral sites upon full disorder in layered $LiMO_2$, only 0.1 f.u. of Li is lost to tetrahedral sites upon disorder in layered $Li_{1.2}M_{0.8}O_2$. This suggests that Li occupancy of tetrahedral sites is a general feature of Li-excess materials, regardless of the amount of cation disorder. The voltage slope increase resulting from the availability of additional tetrahedral Li sites upon disorder is

DOI: 10.1021/acs.chemmater.6b01438
Chem. Mater. 2016, 28, 5373−5383

therefore expected to be less pronounced in Li-excess compounds than in stoichiometric compounds.

4. SUMMARY AND DISCUSSION

This work demonstrated that the voltage slope of cation-disordered rocksalts is a combination of the Li site energy distribution (controlled by Li−M interactions), the effective Li−Va interaction, and the occupancy of tetrahedral sites by Li. It was found that the voltage slope increase upon disorder is generally smaller for high-voltage transition metal oxides than for low-voltage transition metal oxides. Short-range order in practical disordered compounds was found to reduce the voltage slope with respect to a fully random structure by narrowing the width of the site energy distribution as well as by decreasing the availability of tetrahedral sites for Li insertion. Finally, it was found that the additional tetrahedral capacity resulting from disorder is smaller in Li-excess compounds than in stoichiometric compounds.

The inverse correlation between the average voltage and the voltage slope increase upon disorder (Figure 4b) is beneficial for the design of high-capacity disordered rocksalts, as a high average voltage and a moderate voltage slope are simultaneously desirable to access a maximum of capacity at high voltage. This trend can be attributed to the site energy contribution to the voltage slope (Figure 4a, controlled by the effective Li−M interaction) and can be qualitatively explained by the relative positions of the transition metal 3d bands and the oxygen 2p bands. As the atomic number of the transition metal increases, the energy of the metal 3d band decreases, resulting in a higher average voltage (higher $M^{3+/4+}$ extraction energy).[45] Simultaneously, as the energy difference between the metal 3d and oxygen 2p bands decreases, the bonds between transition metal and oxygen atoms become more covalent, leading to a more effective screening of the $M^{3+/4+}$ charge by oxygen electrons.[45] This more effective screening reduces the site energy dependence of Li on its environment, as the site energy difference between Li sites with a large number of transition metal neighbors (resulting in high electrostatic repulsion between Li^{3+} and $M^{3+/4+}$ cations) and Li sites with a small number of transition metal neighbors (resulting in low electrostatic repulsion) decreases (cf. Figure 2b(i)). This in turn leads to a decrease in the voltage slope.

This inverse correlation is consistent with the limited amount of electrochemical data currently available on cation-disordered rocksalts. The only disordered rocksalt that has been partially cycled in the $LiMO_2$ family is disordered $LiTiO_2$, which is formed in operando during cycling of rutile TiO_2.[11,12] Particle nanosizing allows for small diffusion lengths (as low 10 nm[11,12]), which partially compensates for the poor diffusivity of Li in stoichiometric disordered $LiMO_2$ rocksalts.[5,6] After first discharge, during which disordered $LiTiO_2$ is formed, the voltage profile changes and the voltage range upon cycling of 200 mAh/g of Li ($LiTiO_2 \Leftrightarrow Li_{0.4}TiO_2$) is found to be on the order of 2 V.[11,12] The voltage range measured in this compound cannot provide a reliable reference for the open circuit voltage slope of disordered $LiTiO_2$, as only 60% of the capacity can be cycled and as significant hysteresis is present in the voltage profile. Nevertheless, this large voltage slope is in qualitative agreement with our predictions for $LiTiO_2$ (2.8 V slope for octahedral Li insertion in fully disordered $LiTiO_2$). Another low voltage system that undergoes a single redox step, $Li_{1+x}VO_3$ ($V^{4+/5+}$),[7] cycles 1 f.u. of Li in an ∼1.5 V voltage range (based on the discharge profile), at an average voltage of ∼2.5 V (estimated by averaging the charge−discharge voltage profiles). On the other hand, higher voltage redox such as the $Ni^{2+/3+}$ in $Li_{1.2}Ni_{0.33}Ti_{0.33}Mo_{0.14}O_2$[3] and the $M^{3+/4+}$ or $M^{2+/4+}$ redox in $Li_{1.3}Nb_yM_xO_2$ (M = Mn, Fe, Co, Ni)[1] all occur in a voltage range smaller than or equal to 1 V (based on the first charge data). These observations agree with the predicted inverse correlation between the average voltage and the voltage slope of cation-disordered compounds. Interestingly, within the $Li_{1.3}Nb_yM_xO_2$ family (M = Mn, Fe, Co, Ni), it can be observed that the transition metals with the lowest average voltage also have the largest voltage slope and vice versa (based on the transition metal redox as observed on first charge).[1] This general trend is further exemplified by the cation-disordered $Li_{1.3}Nb_{0.3}V_{0.4}O_2$, which cycles at a lower voltage than the other Nb-based compositions owing to the $V^{3+/5+}$ redox and displays a strongly sloped voltage profile.[46] In addition, the voltage profile of the Nb−V material exhibits a pronounced high-voltage plateau that might indicate Li extraction from tetrahedral sites, underlining the importance of tetrahedral Li capacity. Interestingly, repeated cycling at high voltage appears to decrease the amount of tetrahedral Li capacity.[46] While further investigation is required to arrive at a definite conclusion, the Nb−V system seems to demonstrate the effect that short-range order forming upon cycling reduces the concentration of tetrahedral Li sites at the top of charge, as discussed in Section 3.2. We also note that irreversible material degradation by oxygen loss may affect the observed voltage profile,[3] which further complicates the direct comparison of our computational results with measurements. Finally, we note that the low-voltage $Li_{1.211}Mo_{0.467}Cr_{0.3}O_2$ compound, in which Mo undergoes a $4^+/6^+$ redox at an average voltage of ∼2.9 V, also exhibits a large voltage slope (1 formula unit of Li extracted in a 2.4 V window), which further corroborates the inverse correlation between the average voltage and the voltage slope in disordered compounds.

With the exception of Ni, our model predicts that octahedral Li occupancy in high-voltage disordered $LiMO_2$ (Cr, Mn, Fe, Co) does not result in significant capacity above the stability limit of the electrolyte (∼4.5−4.7 V). This is largely due to the smaller spread of site energies in high-voltage transition metals. However, the availability of the tetrahedral site upon delithiation contributes to a high-voltage region at the end of charge. By estimating the stabilization resulting from tetrahedral Li occupancy by the corresponding stabilization in the stoichiometric spinel structure, we find that the voltage increase at the end of charge resulting from tetrahedral Li extraction is on the order 0.3−0.5 V and accounts for 25% of the total capacity in fully disordered $LiMO_2$. This investigation therefore highlights the importance of tetrahedral capacity to the voltage profile of cation-disordered high-voltage transition metal oxides.

In practice, however, cation-disordered rocksalts are not fully random. This was demonstrated for temperature-driven cation disorder of $LiMO_2$ compounds, where the energy of the disordered state is smaller than that of the fully random structure. Short-range order decreases the voltage slope with respect to random cation occupation, by reducing the spread of the local transition metal environment around Li sites as well as by decreasing the number of tetrahedral sites accessible upon delithiation. The degree of short-range order is therefore an important parameter for the design of high-voltage cation-disordered rocksalts. The synthesis of partially disordered compounds, by tailoring the synthesis temperature, could both

DOI: 10.1021/acs.chemmater.6b01438
Chem. Mater. 2016, 28, 5373−5383

leverage the benefits of disordered rocksalts (high mobility at the top of charge) while minimizing the voltage slope increase upon disorder.

In practice, cation-disordered rocksalts require Li excess to sustain macroscopic diffusion ($y \approx 0.2$ in $Li_{1+y}M_{1-y}O_2$).[5,47] The effect of Li excess on the relative amount of octahedral and tetrahedral Li capacity was studied using probability theory. While the absolute amount of available tetrahedral sites increases upon introduction of Li excess, the amount of octahedral capacity lost by cation disorder decreases with the amount of Li excess. This suggests that the Li occupancy of tetrahedral sites is a general feature of Li-excess materials, regardless of the amount of cation disorder. The voltage slope increase resulting from additional availability of tetrahedral sites upon cation disorder is therefore expected to be minimal in Li-excess systems.

5. CONCLUSIONS

In this paper, we developed a model based on first principles to evaluate the voltage slope of stoichiometric cation-disordered lithium transition metal oxides. Our study demonstrated that high-voltage transition metals generally have a lower voltage slope than low-voltage transition metals and therefore have minimal Li capacity above the electrolyte stability limit (with the exception of $LiNiO_2$, which has a high average voltage in its disordered form). Cation disorder, however, leads to occupation of tetrahedral sites by Li, sites which are otherwise inaccessible in the stoichiometric layered structure. The availability of tetrahedral Li sites results in an additional high-voltage region outside the stability range of the electrolyte and can significantly affect the accessible capacity upon cycling.

Short-range order in practical disordered compounds mitigates the voltage slope increase by reducing the amount of local environments around Li sites, as well as by decreasing the availability of tetrahedral sites. Furthermore, the amount of octahedral capacity lost upon disorder decreases with the introduction of Li excess, which is required to enable macroscopic diffusion in disordered rocksalts. Our work therefore provides critical insights for the design of high-capacity Li-excess cation-disordered rocksalts based upon voltage considerations.

■ ASSOCIATED CONTENT

Supporting Information

The Supporting Information is available free of charge on the ACS Publications website at DOI: 10.1021/acs.chemmater.6b01438.

Expressing the site energy in terms of effective pair interactions, fitting method for J^{Li-Va}, J^{Li-M}, and J^{Va-M}, accuracy of the pair term approximation, and determining ΔV^{tet} from the spinel structure (PDF)

■ AUTHOR INFORMATION

Notes

The authors declare no competing financial interest.

■ ACKNOWLEDGMENTS

This work was inspired by cathode development funded by the Robert Bosch Corporation and by Umicore Specialty Oxides and Chemicals. Its theory development was funded by the NorthEast Center for Chemical Energy Storage (NECCES), an Energy Frontier Research Center funded by the U.S. Department of Energy, Office of Science, Basic Energy Sciences, under Award No. DE-SC0012583. Computational resources from the National Energy Research Scientific Computing Center (NERSC) and from the Extreme Science and Engineering Discovery Environment (XSEDE) are gratefully acknowledged.

■ REFERENCES

(1) Yabuuchi, N.; Takeuchi, M.; Nakayama, M.; Shiiba, H.; Ogawa, M.; Nakayama, K.; Ohta, T.; Endo, D.; Ozaki, T.; Inamasu, T.; Sato, K.; Komaba, S. High-Capacity Electrode Materials for Rechargeable Lithium Batteries: Li3NbO4-Based System with Cation-Disordered Rocksalt Structure. *Proc. Natl. Acad. Sci. U. S. A.* **2015**, *112*, 7650−7655.

(2) Wang, R.; Li, X.; Liu, L.; Lee, J.; Seo, D.-H.; Bo, S.-H.; Urban, A.; Ceder, G. A Disordered Rock-Salt Li-Excess Cathode Material with High Capacity and Substantial Oxygen Redox Activity: Li1.25Nb0.25Mn0.5O2. *Electrochem. Commun.* **2015**, *60*, 70−73.

(3) Lee, J.; Seo, D.-H.; Balasubramanian, M.; Twu, N.; Li, X.; Ceder, G. A New Class of High Capacity Cation-Disordered Oxides for Rechargeable Lithium Batteries: Li−Ni−Ti−Mo Oxides. *Energy Environ. Sci.* **2015**, *8*, 3255−3265.

(4) Glazier, S. L.; Li, J.; Zhou, J.; Bond, T.; Dahn, J. R. Characterization of Disordered Li (1+X)Ti2xFe(1−3x)O2 as Positive Electrode Materials in Li-Ion Batteries Using Percolation Theory. *Chem. Mater.* **2015**, *27*, 7751−7756.

(5) Lee, J.; Urban, A.; Li, X.; Su, D.; Hautier, G.; Ceder, G. Unlocking the Potential of Cation-Disordered Oxides for Rechargeable Lithium Batteries. *Science* **2014**, *343*, 519−522.

(6) Urban, A.; Lee, J.; Ceder, G. The Configurational Space of Rocksalt-Type Oxides for High-Capacity Lithium Battery Electrodes. *Adv. Energy Mater.* **2014**, *4*, 1400478.

(7) Pralong, V.; Gopal, V.; Caignaert, V.; Duffort, V.; Raveau, B. Lithium-Rich Rock-Salt-Type Vanadate as Energy Storage Cathode: Li2−xVO3. *Chem. Mater.* **2012**, *24*, 12−14.

(8) Lyu, Y.; Ben, L.; Sun, Y.; Tang, D.; Xu, K.; Gu, L.; Xiao, R.; Li, H.; Chen, L.; Huang, X. Atomic Insight Into Electrochemical Inactivity of Lithium Chromate (LiCrO2): Irreversible Migration of Chromium Into Lithium Layers in Surface Regions. *J. Power Sources* **2015**, *273*, 1218−1225.

(9) Bo, S.; Li, X.; Toumar, A. J.; Ceder, G. Layered-to-Rocksalt Transformation in Desodiated NaxCrO2 (X 0.4). *Chem. Mater.* **2016**, *28*, 1419−1429.

(10) Ozawa, K.; Nakao, Y.; Wang, L.; Cheng, Z.; Fujii, H.; Hase, M.; Eguchi, M. Structural Modifications Caused by Electrochemical Lithium Extraction for Two Types of Layered LiVO2 (R3m). *J. Power Sources* **2007**, *174*, 469−472.

(11) Baudrin, E.; Cassaignon, S.; Koelsch, M.; Jolivet, J.; Dupont, L.; Tarascon, J. Structural Evolution During the Reaction of Li with Nano-Sized Rutile Type TiO2 at Room Temperature. *Electrochem. Commun.* **2007**, *9*, 337−342.

(12) Wang, D.; Choi, D.; Yang, Z.; Viswanathan, V. V.; Nie, Z.; Wang, C.; Song, Y.; Zhang, J.-G.; Liu, J. Synthesis and Li-Ion Insertion Properties of Highly Crystalline Mesoporous Rutile TiO2. *Chem. Mater.* **2008**, *20*, 3435−3442.

(13) Hwang, S.; Chang, W.; Kim, S. M.; Su, D.; Kim, D. H.; Lee, J. Y.; Chung, K. Y.; Stach, E. A. Investigation of Changes in the Surface Structure of LixNi 0.8Co0.15Al0.05O2 Cathode Materials Induced by the Initial Charge. *Chem. Mater.* **2014**, *26*, 1084−1092.

(14) Zheng, S.; Huang, R.; Makimura, Y.; Ukyo, Y.; Fisher, C. A. J.; Hirayama, T.; Ikuhara, Y. Microstructural Changes in LiNi0.8-Co0.15Al0.05O2 Positive Electrode Material During the First Cycle. *J. Electrochem. Soc.* **2011**, *158*, A357−A362.

(15) Zheng, J.; Xu, P.; Gu, M.; Xiao, J.; Browning, N. D.; Yan, P.; Wang, C.; Zhang, J.-G. Structural and Chemical Evolution of Li- and Mn-Rich Layered Cathode Material. *Chem. Mater.* **2015**, *27*, 1381−1390.

DOI: 10.1021/acs.chemmater.6b01438
Chem. Mater. 2016, 28, 5373−5383

(16) Yan, P.; Nie, A.; Zheng, J.; Zhou, Y.; Lu, D.; Zhang, X.; Xu, R.; Belharouak, I.; Zu, X.; Xiao, J.; Amine, K.; Liu, J.; Gao, F.; Shahbazian-Yassar, R.; Zhang, J.-G.; Wang, C.-M. Evolution of Lattice Structure and Chemical Composition of the Surface Reconstruction Layer in Li1.2Ni 0.2Mn0.6O2 Cathode Material for Lithium Ion Batteries. *Nano Lett.* **2015**, *15*, 514−522.
(17) Boulineau, A.; Simonin, L.; Colin, J.-F.; Canévet, E.; Daniel, L.; Patoux, S. Evolutions of Li1.2Mn0.61Ni0.18Mg0.01O2 During the Initial Charge/Discharge Cycle Studied by Advanced Electron Microscopy. *Chem. Mater.* **2012**, *24*, 3558−3566.
(18) Jung, S.-K.; Gwon, H.; Hong, J.; Park, K.-Y.; Seo, D.-H.; Kim, H.; Hyun, J.; Yang, W.; Kang, K. Understanding the Degradation Mechanisms of LiNi0.5Co0.2Mn0.3O2 Cathode Material in Lithium Ion Batteries. *Adv. Energy Mater.* **2014**, *4*, 1300787.
(19) Genevois, C.; Koga, H.; Croguennec, L.; Ménétrier, M.; Delmas, C.; Weill, F. Insight Into the Atomic Structure of Cycled Lithium-Rich Layered Oxide Li 1.20Mn0.54Co0.13Ni0.13O2 Using HAADF STEM and Electron Nanodiffraction. *J. Phys. Chem. C* **2015**, *119*, 75−83.
(20) Tarascon, J. M.; Armand, M. Issues and Challenges Facing Rechargeable Lithium Batteries. *Nature* **2001**, *414*, 359−367.
(21) Hewston, T. A.; Chamberland, B. L. A Survey of First-Row Ternary Oxides LiMO2 (M = Sc-Cu). *J. Phys. Chem. Solids* **1987**, *48*, 97−108.
(22) Chang, S. H.; Kang, S.-G.; Song, S.-W.; Yoon, J.-B.; Choy, J.-H. Crystal Structure and Spectroscopic Properties of LixNi1-yTiyO2 and Their Electrochemical Behavior. *Solid State Ionics* **1996**, *86*−*88*, 171−175.
(23) Küzma, M.; Dominko, R.; Meden, A.; Makovec, D.; Bele, M.; Jamnik, J.; Gaberšček, M. Electrochemical Activity of Li2FeTiO4 and Li2MnTiO4 as Potential Active Materials for Li Ion Batteries: a Comparison with Li2NiTiO4. *J. Power Sources* **2009**, *189*, 81−88.
(24) Yang, M.; Zhao, X.; Bian, Y.; Ma, L.; Ding, Y.; Shen, X. Cation Disordered Rock Salt Phase Li2CoTiO4 as a Potential Cathode Material for Li-Ion Batteries. *J. Mater. Chem.* **2012**, *22*, 6200−6205.
(25) Kang, K.; Carlier, D.; Reed, J.; Arroyo, E. M.; Ceder, G.; Croguennec, L.; Delmas, C. Synthesis and Electrochemical Properties of Layered Li0.9Ni0.45Ti0.55O2. *Chem. Mater.* **2003**, *15*, 4503−4507.
(26) Cowley, J. M. Short- and Long-Range Order Parameters in Disordered Solid Solutions. *Phys. Rev.* **1960**, *120*, 1648−1657.
(27) Breger, J.; Meng, Y. S.; Hinuma, Y.; Kumar, S.; Kang, K.; Shao-Horn, Y.; Ceder, G.; Grey, C. P. Effect of High Voltage on the Structure and Electrochemistry of LiNi 0.5Mn 0.5O 2: a Joint Experimental and Theoretical Study. *Chem. Mater.* **2006**, *18*, 4768−4781.
(28) Croguennec, L.; Palacín, M. R. Recent Achievements on Inorganic Electrode Materials for Lithium-Ion Batteries. *J. Am. Chem. Soc.* **2015**, *137*, 3140−3156.
(29) Sanchez, J. M.; Ducastelle, F.; Gratias, D. Generalized Cluster Description of Multicomponent Systems. *Phys. A* **1984**, *128*, 334−350.
(30) De Fontaine, D. Cluster Approach to Order-Disorder Transformations in Alloys. *Solid State Phys.* **1994**, *47*, 33−176.
(31) Wolverton, C.; De Fontaine, D. Cluster Expansions of Alloy Energetics in Ternary Intermetallics. *Phys. Rev. B: Condens. Matter Mater. Phys.* **1994**, *49*, 8627−8642.
(32) Nelson, L. J.; Hart, G. L. W.; Zhou, F.; Ozoliņš, V. Compressive Sensing as a Paradigm for Building Physics Models. *Phys. Rev. B: Condens. Matter Mater. Phys.* **2013**, *87*, 035125.
(33) Van der Ven, A.; Thomas, J. C.; Xu, Q.; Bhattacharya, J. Linking the Electronic Structure of Solids to Their Thermodynamic and Kinetic Properties. *Mathematics and Computers in Simulation* **2010**, *80*, 1393−1410.
(34) Arroyo y de Dompablo, M. E.; Ceder, G. First-Principles Calculations on LixNiO2: Phase Stability and Monoclinic Distortion. *J. Power Sources* **2003**, *119*−*121*, 654−657.
(35) Van der Ven, A.; Aydinol, M. K.; Ceder, G.; Kresse, G.; Hafner, J. First-Principles Investigation of Phase Stability in Li_XCoO_2. *Phys. Rev. B: Condens. Matter Mater. Phys.* **1998**, *58*, 2975−2987.
(36) Wolverton, C.; Zunger, A. Cation and Vacancy Ordering in Li_XCoO_2. *Phys. Rev. B: Condens. Matter Mater. Phys.* **1998**, *57*, 2242−2252.
(37) Asta, M.; Wolverton, C.; De Fontaine, D.; Dreyssé, H. Effective Cluster Interactions From Cluster-Variation Formalism. *Phys. Rev. B: Condens. Matter Mater. Phys.* **1991**, *44*, 4907−4913.
(38) Perdew, J. P.; Burke, K.; Ernzerhof, M. Generalized Gradient Approximation Made Simple. *Phys. Rev. Lett.* **1996**, *77*, 3865−3868.
(39) Perdew, J. P.; Burke, K.; Ernzerhof, M. Generalized Gradient Approximation Made Simple - Errata. *Phys. Rev. Lett.* **1997**, *78*, 1396.
(40) Anisimov, V. I.; Zaanen, J.; Andersen, O. K. Band Theory and Mott Insulators: Hubbard U Instead of Stoner I. *Phys. Rev. B: Condens. Matter Mater. Phys.* **1991**, *44*, 943−954.
(41) Jain, A.; Hautier, G.; Moore, C. J.; Ping Ong, S.; Fischer, C. C.; Mueller, T.; Persson, K. A.; Ceder, G. A High-Throughput Infrastructure for Density Functional Theory Calculations. *Comput. Mater. Sci.* **2011**, *50*, 2295−2310.
(42) Abdellahi, A.; Urban, A.; Dacek, S.; Ceder, G. The Effect of Cation Disorder on the Average Li Intercalation Voltage of Transition Metal Oxides. *Chem. Mater.* **2016**, *28*, 3659−3665.
(43) Urban, A.; Matts, I.; Abdellahi, A.; Ceder, G. Computational Design and Preparation of Cation-Disordered Oxides for High-Energy-Density Li-Ion Batteries. *Adv. Energy Mater.* **2016**, DOI: 10.1002/aenm.201600488.
(44) Jarvis, K. A.; Deng, Z.; Allard, L. F.; Manthiram, A.; Ferreira, P. J. Atomic Structure of a Lithium-Rich Layered Oxide Material for Lithium-Ion Batteries: Evidence of a Solid Solution. *Chem. Mater.* **2011**, *23*, 3614−3621.
(45) Aydinol, M. K.; Kohan, A. F.; Ceder, G. Ab Initio Calculation of the Intercalation Voltage of Lithium-Transition-Metal Oxide Electrodes for Rechargeable Batteries. *J. Power Sources* **1997**, *68*, 664−668.
(46) Yabuuchi, N.; Takeuchi, M.; Komaba, S.; Ichikawa, S.; Ozaki, T.; Inamasu, T. Synthesis and Electrochemical Properties of Li1.3Nb0.3-V0.4O2 as a Positive Electrode Material for Rechargeable Lithium Batteries. *Chem. Commun.* **2016**, *52*, 2051−2054.
(47) Urban, A.; Lee, J.; Ceder, G. The Configurational Space of Rocksalt-Type Oxides for High-Capacity Lithium Battery Electrodes. *Adv. Energy Mater.* **2014**, *4*, 1400478.

DOI: 10.1021/acs.chemmater.6b01438
Chem. Mater. 2016, 28, 5373−5383